Dowel Laminated Timber Elements Manufactured using Compressed Wood Dowels

Conan O'Ceallaigh[1], Annette M. Harte[1], Patrick J. McGetrick[1]
[1]College of Science and Engineering & Ryan Institute, National University of Ireland Galway, University Road, Galway, Ireland
Email; conan.oceallaigh@nuigalway.ie, annette.harte@nuigalway.ie, patrick.mcgetrick@nuigalway.ie

ABSTRACT: In recent years, there has been an increased focus on the environmental impacts of construction and a movement towards more sustainable construction products. The use of timber as a structural material has grown and it has been deemed to be one of the leading materials of choice in the future as a sustainable construction product that not only has a low carbon footprint but also acts as a carbon store for the lifetime of the structural component. To further improve the environmental performance of timber construction, it is beneficial to reduce the use of adhesives, particularly when manufacturing laminated engineered wood products. This study numerically investigates the structural behaviour of dowel laminated timber (DLT) elements which are laminated with compressed wood dowels instead of adhesives. A parametric study is carried out to examine the influence of dowel diameter and spacing on the stiffness and maximum load capacity of the DLT members. The numerical model incorporates orthotropic, linear elastic materials in tension and linear elastic-plastic materials in compression. Furthermore, damage initiation criteria in the respective material directions are utilised to determine the failure behaviour of the structural elements. The results show that the dowel diameter and spacing have a significant influence on the maximum load capacity and stiffness of the DLT members. The predicted failure behaviour of the numerical model comprises a combination of dowel bending, dowel-timber embedment and tensile fracture of the bottom tensile laminate. The numerical model will allow for an optimised dowel arrangement to be manufactured and experimentally tested.

KEYWORDS: Compressed wood dowels; Dowel Laminated Timber (DLT); Engineered Wood Products; Numerical modelling; Parametric study.

1 INTRODUCTION

The construction industry has seen an increased focus in recent years on global warming and the impact of human activities on the built environment. This has mobilised the industry to achieve new standards in environmental performance for our buildings as the construction industry aims to reduce its carbon footprint. It is not surprising that a considerable body of research into the development of timber structures as a sustainable alternative to steel and concrete has occurred in recent years. Many studies have investigated different technologies and materials to develop highly engineered timber products or engineered wood products (EWPs) that can achieve significant load-bearing capacity and stiffness allowing timber buildings to achieve new heights [1,2].

Timber is one of the oldest building materials and is naturally renewable when sustainably grown. As a result, timber is set to be the leading material of choice in the future as a sustainable construction product that not only has a low carbon footprint but also acts as a carbon store for the lifetime of the structural component. One of the significant advances in engineered wood technology has been glued laminating technology to form products such as glulam and cross-laminated timber (CLT), which comprises adhesively bonded timber boards to form a robust, reliable engineered wood panel product that can be used in floor, roof and wall applications [2–6]. The purpose of this research is to investigate the use of dowel laminating technology to form connections between adjacent timber laminations. The process typically involves the use of hardwood dowels positioned within drilled holes to form a tight fit connection between adjacent laminations as shown in Figure 1-1 The use of such technology has been successfully utilised to form dowel laminated timber (DLT) panels and beams using a variety of different species [7–10]. The use of such technology ultimately reduces the use of adhesives in EWPs and further improves the environmental credentials. The efficiency of the connection is reduced when compared to adhesively bonded EWPs and as such, it is important to understand the parameters that affect the strength and stiffness of such connections and the ultimate strength and stiffness of the developed DLT product.

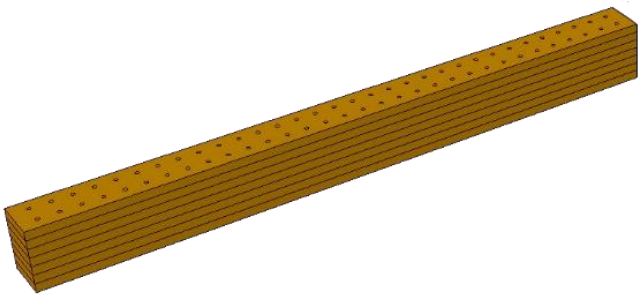

Figure 1-1. Typical dowel laminated timber (DLT) beam connected with hardwood timber dowels.

In this study, the use of compressed timber dowels is explored as a potential alternative to hardwood dowels. Compressed wood (CW) dowels are made from softwoods, which are compressed under heat and pressure to enhance their structural properties, and have been shown to have excellent properties when used in timber connections [11–14]. A finite element (FE) model is developed to predict the structural behaviour of DLT beams utilising CW dowels. The numerical model is developed in Abaqus software and utilises a UMAT

subroutine based on the Hashin damage model to determine the damage initiation criteria within the timber boards and the CW dowels. The model has been formulated to consider damage in the longitudinal direction or along the grain of the timber and in the perpendicular to the grain direction separately. Additionally, the failure criteria under tension and compression are treated differently to accurately model the behaviour of timber under such loading modes and to determine the failure behaviour of the simulated EWPs.

2 DOWEL LAMINATED TIMBER

2.1 Introduction

The use of dowel laminated technology has been the subject of a number of studies in recent years as an alternative to glued laminating technology to further improve the environmental performance of EWPs [7–10,15–19]. There have been significant advances in this technology and a number of commercial products are available and in use in several large timber structures across the world [7,20].

In this study, Sitka spruce timber grown in Ireland is used as the primary structural material and the influence of a series of design parameters, namely, dowel diameter and dowel spacing, on the structural behaviour of a DLT beam is investigated.

Three dowel diameters, 10 mm, 15 mm and 20 mm and three dowel spacing distances of 50 mm, 75 mm and 100 mm will be examined using a numerical model to determine the structural behaviour. The naming convention of each specimen is presented in Table 1.

Table 1. Numerical models and design parameters

Numerical model Specimen	Dowel Diameter (mm)	Dowel Spacing (mm)
DLT-D10-S50	10	50
DLT-D15-S50	15	50
DLT-D20-S50	20	50
DLT-D10-S75	10	75
DLT-D15-S75	15	75
DLT-D20-S75	20	75
DLT-D10-S100	10	100
DLT-D15-S100	15	100
DLT-D20-S100	20	100

2.2 Beam geometry

The beam geometry under investigation in this study is presented in Figure 2-1. The beam comprises three timber laminations measuring 1140 mm in length and a cross-section of 20 mm x 60 mm. The three timber laminations are combined to form a final cross-section of 60 mm x 60 mm and a length of 1140 mm with the dowel diameter and spacing varying as presented in Table 1. The specimen geometry was chosen based on the criteria for the bending test specified in EN 408 [21]. This test standard specifies four-point bending over a test span of 18 times the specimen depth. As a result, the test specimen is supported over a test span of 1080 mm with point loads at 360 mm from each support. Steel plates (60 mm x 30 mm x 10 mm) are positioned at the support points and load points as specified by EN 408 [21]. As seen in Figure 2-1, the midspan of each beam is represented by a red dotted line. It is at this location that the global vertical displacement of the beam is determined for a given load until failure occurs.

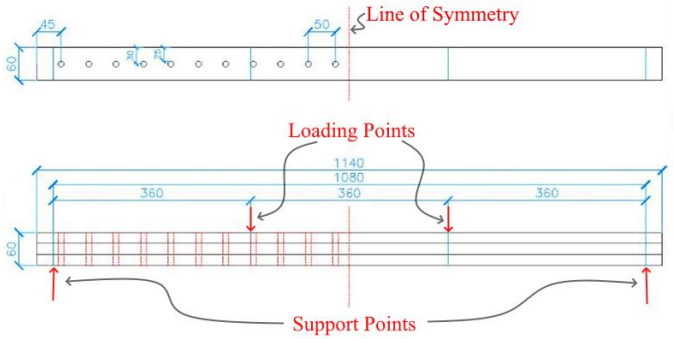

Figure 2-1. DLT geometry for the 10mm diameter dowels and the dowel spacing of 50mm (DLT-D10-S50). Dimensions in mm.

2.3 Timber

For the purpose of this study, Sitka spruce, grown in Ireland, is the primary material under investigation. The timber material is modelled as an orthotropic elastic material in Abaqus FEA software. The Sitka spruce material tested experimentally by O'Ceallaigh et al. [22–24] was graded to strength class C16. The standard EN 338 [25] provides a mean value of 8000 MPa for the elastic modulus of C16 timber in the longitudinal direction; however, it was experimentally determined by O'Ceallaigh et al. [22–24] that a longitudinal elastic modulus of 9200 N/mm^2 is more representative of the actual elastic properties. For simplicity, the radial and tangential properties were assumed to be equal and the tangential value has been selected for the material properties perpendicular to the grain. The tangential elastic moduli (radial and tangential) directions were not measured experimentally; however, Bodig & Jayne [26] expressed a general relationship between the elastic modulus, E and shear modulus, G in the three material directions. Although these ratios are not without their inaccuracies, they are widely accepted for modelling the orthotropic properties of timber.

2.4 Compressed wood dowels

Typically, hardwood dowels have been used in the manufacture of DLT products, however, in this study, compressed wood dowels are used. CW is a type of modified wood material that has been shown to have superior structural properties to natural timber and has proved to be an environmentally friendly alternative to metallic fasteners in timber connections [12,14,27–29]. The compressed wood used in this study was produced by a process of thermo-mechanical compression of softwood timber to increase its density, strength, stiffness, hardness and to reduce its porosity [30,31].

Compressed wood in the form of dowels showed good properties when tested in shear and when compared with other standard hardwood dowels and their use in DLT elements is of interest to the industry [31]. The modification process involves a simultaneous increase in temperature and the application of pressure. As the temperature increases, the timber may be easily compressed reducing the void space between the cell walls, increasing the density significantly and improving many structural properties of the timber. As the density of the timber is increased, a proportional improvement in stiffness, yield load and maximum load is expected. However, in contrast, the plastic modulus has been shown to decrease in some species

[32]. The compressed wood, with enhanced structural properties compared to standard hardwood dowel, also has a spring-back or shape-recovery property that means it will expand over time resulting in a tight fit connection that may be a beneficial characteristic in many structural timber engineering applications, particularly DLT beams and panels [33].

3 NUMERICAL MODELING

3.1 Finite element formulation

In this section, the constitutive model used to simulate the failure behaviour of Sitka spruce DLT members fastened with CW dowels is presented. A three-dimensional finite element model is developed, incorporating a UMAT subroutine to determine the total strain and associated damage experienced in timber elements when subjected to external loading. The elastic component of the timber, CW dowels and steel plates follows the generalised Hooke's law. The material behaviour of the timber and CW dowels are assumed to be orthotropic with a stronger and stiffer response along the fibre direction and reduced properties perpendicular to the grain. The material properties for both the timber and CW are presented in Table 2. For simplicity, the radial and tangential directions of the timber are considered equal in this model. The subscript '*L*' and '*T*' represent the longitudinal and transverse materials directions for timber. E_L and E_T represent the elastic modulus in the longitudinal or parallel to the grain direction and the transverse or perpendicular to the grain direction, respectively. G_{LT} and G_{TT} are the shear moduli and v_{LT} and v_{TT} are the Poisson's ratios.

Similar to the elastic properties, the strength characteristics are also assumed to be orthotropic. The values are presented in Table 2 with superscripts '*t*' and '*c*' which refer to the tension and compression, respectively. For example, $\sigma_L{}^t$ represents the value of the longitudinal failure stress when loaded in tension. The shear failure stress, τ_{LT} is also presented. G_T and G_L represent the fracture energies in the transverse and longitudinal directions, respectively and to improve convergence, a viscosity parameter, η is utilised in the user subroutine to regularise the damage variables and control the rate of damage.

$$f_L = \sqrt{\frac{\varepsilon_{11}^t}{\varepsilon_{11}^c}(\varepsilon_{11})^2 + \left(\varepsilon_{11}^t - \frac{(\varepsilon_{11}^t)^2}{\varepsilon_{11}^c}\right)\varepsilon_{11}} > \varepsilon_{11}^t \quad (1)$$

where

$$\varepsilon_{11}^t = {\sigma_L^t}/{C_{11}};\ \varepsilon_{11}^c = {\sigma_L^c}/{C_{11}} \quad (2)$$

where *Cij* are the components of the elastic matrix in the undamaged state. When Eq. (1) is satisfied, the damage variable d_L is determined according to Eq. (3).

$$d_L = 1 - \frac{\varepsilon_{11}^t}{f_L} e^{(-C_{11}\varepsilon_{11}^t(f_L - \varepsilon_{11}^t)L_c/G_L)} \quad (3)$$

where L_C and G_L are the characteristic element length and the fracture energy, respectively.

The corresponding equations for the perpendicular to the grain direction are produced similarly in Eqs. (4), (5) and (6),

$$f_T = \sqrt{\frac{\varepsilon_{22}^t}{\varepsilon_{22}^c}(\varepsilon_{22})^2 + \left(\varepsilon_{22}^t - \frac{(\varepsilon_{22}^t)^2}{\varepsilon_{22}^c}\right)\varepsilon_{22} + \left(\frac{\varepsilon_{22}^t}{\varepsilon_{12}^\tau}\right)^2(\varepsilon_{12})^2} > \varepsilon_{22}^t \quad (4)$$

where

$$\varepsilon_{22}^t = {\sigma_T^t}/{C_{22}};\quad \varepsilon_{22}^c = {\sigma_T^c}/{C_{22}};\quad \varepsilon_{12}^\tau = {\tau_{LT}^t}/{C_{44}} \quad (5)$$

When Eq. (4) is satisfied, the damage variable d_T is determined according to Eq. (6).

$$d_T = 1 - \frac{\varepsilon_{22}^t}{f_T} e^{(-C_{22}\varepsilon_{22}^t(f_T - \varepsilon_{22}^t)L_c/G_T)} \quad (6)$$

The occurrence of damage is established when the elastic matrix is updated to form an effective elasticity matrix (C_d) which has terms reduced by including the two damage variables d_L and d_T as shown in Eq. (7).

$$C_d = \begin{bmatrix} (1-d_L)C_{11} & (1-d_L)(1-d_T)C_{12} & (1-d_L)C_{13} & 0 & 0 & 0 \\ & (1-d_T)C_{22} & (1-d_T)C_{23} & 0 & 0 & 0 \\ & & C_{33} & 0 & 0 & 0 \\ & Symmetric & & (1-d_L)(1-d_T)C_{44} & 0 & 0 \\ & & & & C55 & 0 \\ & & & & & C66 \end{bmatrix} \quad (7)$$

The damage initiation criteria utilised in this model are based on the Hashin damage model which has been utilised in a series of studies to determine the failure behaviour of timber elements [34–38]. The damage initiation criteria are expressed in terms of strains and are treated differently for tension and compression strains however, one affects the other and if the strains are significant and cause partial or full damage (damage variable greater than zero) both tensile and compressive responses are affected. For example, damage in the longitudinal direction is initiated when the following criterion is achieved.

In the user subroutine, the stresses are then updated according to Eq. (8)

$$\sigma = C_d : \varepsilon \quad (8)$$

The differentiation of the above equation is used to determine the Jacobian matrix as presented in Eq. (9).

$$\frac{\partial \sigma}{\delta \varepsilon} = C_d + \frac{\delta C_d}{\delta \varepsilon} : \varepsilon$$

$$= C_d + \left(\frac{\delta C_d}{\delta d_T} : \varepsilon\right)\left(\frac{\delta d_T}{\delta f_T}\frac{\delta f_T}{\delta \varepsilon}\right) + \left(\frac{\delta C_d}{\delta d_L} : \varepsilon\right)\left(\frac{\delta d_L}{\delta f_L}\frac{\delta f_L}{\delta \varepsilon}\right) \quad (9)$$

Furthermore, to improve the convergence, a viscosity parameter, η is utilised in the user subroutine to regularise the damage variables and control the rate of damage using the following Eqs (10) and (11).

$$\dot{d}_L^r = \frac{1}{\eta}(d_L - d_L^r) \quad (10)$$

$$\dot{d}_T^r = \frac{1}{\eta}(d_T - d_T^r) \quad (11)$$

where all parameters are as presented before but the superscript 'r' indicates regularised and the accent '˙' indicates rate. The regularised damage variable is updated for each time step in the analysis.

4 FINITE ELEMENT MODEL

This section presents the development of the model in Abaqus FEA software.

4.1 Model Geometry

The geometry of the DLT members, which are subjected to four-point bending in accordance with EN 408 [21], has been modelled in Abaqus FE software. As presented in Figure 4-1, the model utilises half symmetry to reduce the number of elements and computational time to solve the model. A symmetric boundary condition (BC) at the midspan is used to achieve this. The DLT member is supported on a steel plate (60 mm x 30 mm x 10 mm) at one end to represent the support condition. As this end support is simply supported, the plate is free to rotate about its central axis. A similar steel plate is also used to apply the vertical load on the top surface of the DLT beam. In relation to the steel-timber interaction, hard contact is defined between the surface of the beam and the steel plates with a tangential friction coefficient of 0.4. Each DLT member in this study comprises three laminations, each of which are assigned material properties in an orthotropic coordinate system. In relation to the timber-timber interaction between each timber lamination, again, hard contact is defined with a tangential friction coefficient of 0.4.

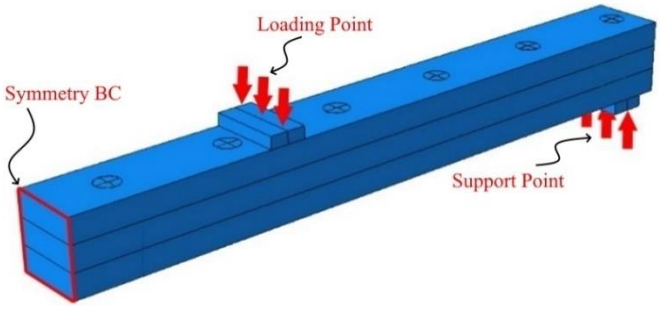

Figure 4-1. Numerical model geometry subjected to four-point bending utilising half symmetry (DLT-D20-S100).

The only differences in the developed models are the dowel diameter and spacing. DLT-D20-S100 is presented in Figure 4-1 and has a dowel diameter of 20 mm and a dowel spacing of 100 mm. The CW dowel-timber interaction is assumed to be similar to the timber-timber interaction, which is a conservative assumption in the absence of more experimental data.

The models were subjected to a mesh sensitivity study prior to performing the parametric study to provide accurate results in a reasonable time frame. All components in the model were meshed with 8-noded C3D8 elements.

4.2 Material data

The material data used in this model for the timber and the CW dowels are presented in Table 2. The steel plates are modelled as linear elastic material with an elastic modulus of 210 GPa and a Poisson's ratio of 0.3. The timber material properties presented in Table 2 are based on a study by O'Ceallaigh et al. [22–24] and the material properties of the CW dowel material are based on findings by O'Ceallaigh et al. [13,30].

Table 2. FEM UMAT Material properties

Property	Timber	CW Dowels	Unit
E_L	9222	28000	MPa
E_T	663	2240	MPa
G_{LT}	659	2000	MPa
G_{TT}	66	200	MPa
ν_{LT}	0.038	0.48	-
ν_{TT}	0.558	0.35	-
σ_L^t	24	130	MPa
σ_L^c	36	130	MPa
σ_T^t	3	80	MPa
σ_T^c	6.3	80	MPa
τ_{LT}	6.9	6.9	MPa
G_T	30	30	N/mm
G_L	60	60	N/mm
η	0.0001	0.0001	-

The definition of the symbols and the notation has been presented in Section 3.1.

5 NUMERICAL RESULTS

In this section, the results of the numerical simulation of the DLT specimens are presented. The load-displacement behaviour simulated by the numerical model is presented along with the maximum load (F_{max}) from each model, the displacement at maximum load and the elastic modulus. The elastic modulus is determined on the linear proportion of the graph between 10% and 40% of the maximum load. These results are presented in Table 3.

Table 3. Numerical model results

Numerical Model Specimen	F_{max} (N)	Displacement (mm)	Elastic modulus (N/mm^2)
DLT-D10-S50	6829	52.2	4517
DLT-D15-S50	6818	57.2	4662
DLT-D20-S50	6245	57.4	4233
DLT-D10-S75	6234	50.3	4120
DLT-D15-S75	6262	46.6	4277
DLT-D20-S75	6058	47.9	4227
DLT-D10-S100	5870	47.2	3910
DLT-D15-S100	6130	48.8	4222
DLT-D20-S100	5943	47.9	4187

The numerical model simulated the load-displacement curves with failure modes comprising a combination of dowel bending, dowel-timber embedment and tensile fracture of the

bottom tensile laminate. The results are graphically presented in Figure 5-1, Figure 5-2 and Figure 5-3 for the dowel diameter of 10 mm, 15 mm and 20 mm, respectively. In each figure, a line indicated as 'Glulam' represents the theoretical stiffness of a glued beam with an elastic modulus of 9200 N/mm^2 to allow for comparison with the stiffness of the DLT members. In Figure 5-1, it is clear that decreasing the spacing between the 10 mm dowels has a positive impact on strength and stiffness. Reducing the spacing from 100 mm to 50 mm results in an increase in strength and stiffness of 16% and 15% respectively.

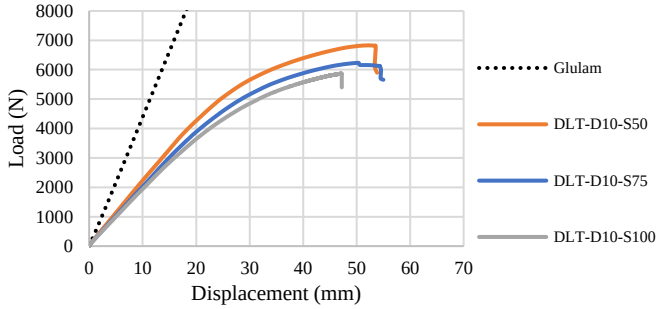

Figure 5-1. Numerical load-displacement curves for specimens with 10 mm diameter dowels (D-10 Series).

When the dowel diameter is increased to 15 mm, as seen in Figure 5-2, an improvement in strength and stiffness was observed for each dowel spacing studied. The influence of dowel spacing was not as significant as was observed for the 10 mm dowels with increases of 11% and 10% in strength and stiffness, respectively.

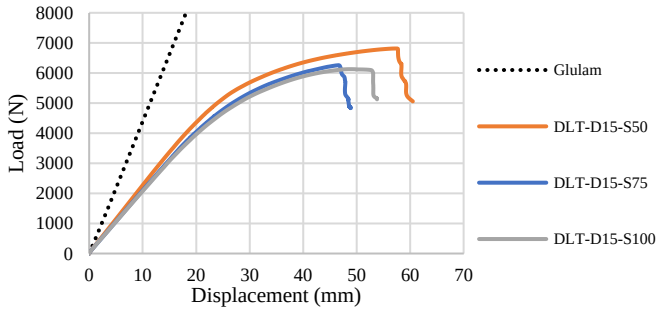

Figure 5-2. Numerical load-displacement curves for specimens with 15 mm diameter dowels (D-15 Series).

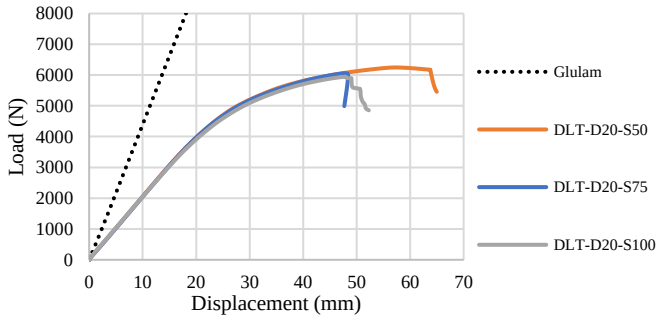

Figure 5-3. Numerical simulated load-displacement curves for specimens with 20 mm diameter dowels (D-20 Series).

Finally, for the 20 mm dowels, presented in Figure 5-3, very consistent load-displacement behaviour was observed. However, increasing the dowel diameter to 20 mm has a negative influence on the strength and stiffness. The results indicate that load-displacement behaviour is governed by the timber substrate and further studies should examine the effect for larger cross-sections.

5.1 Influence of dowel diameter and spacing

The influence of dowel spacing for all specimens studied can be seen in Figure 5-4 and Figure 5-5. In Figure 5-4, it can be seen that the 50 mm spacing provided the highest loads for the 10mm and 15 mm dowel diameters but this reduced for the 20 mm dowels. This may be an issue with reduced edge distances and may not be the case for larger cross-sections.

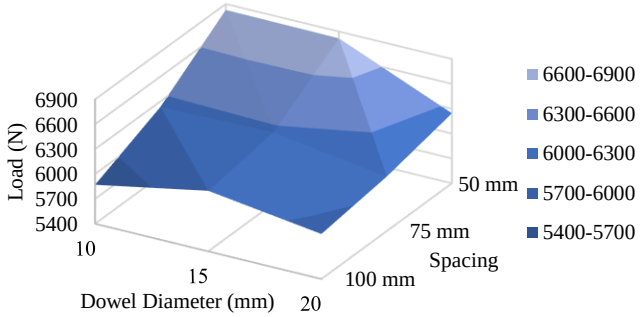

Figure 5-4. The influence of dowel diameter and dowel spacing on maximum load (F_{max}).

In Figure 5-5, the influence of dowel diameter and spacing on the observed elastic modulus for all specimens studied can be seen. It is clear that as the dowel diameter is increased from 10 mm to 15 mm, there was a positive influence on elastic modulus and associated stiffness of the DLT beam. The maximum stiffness was observed for the 15 mm CW dowels with a spacing of 50 mm.

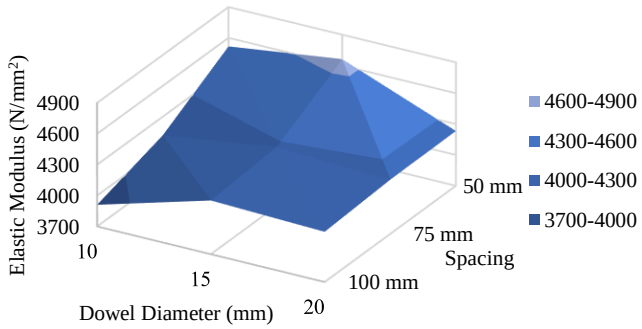

Figure 5-5. The influence of dowel diameter and dowel spacing on elastic modulus.

6 CONCLUSION

The numerical model results for DLT members connected using CW dowels have been presented for dowel diameters of 10 mm, 15 mm, and 20 mm with spacings arrangements of 50 mm, 75 mm and 100 mm.

Typically, increasing the dowel diameter and reducing the dowel spacing have a positive influence on strength and stiffness. This was true for the 10 mm and 15 mm dowel diameters. However, the 20 mm dowels appear to have very consistent behaviour for all spacing arrangements examined, their strength and stiffness values were less than those of the 15 mm dowels. Further studies should examine the effect of larger cross-sections and the influence of edge spacing and end distances on such members.

When examining the load-displacement behaviour, in all cases, it was clear that the spacing had less of an effect on the strength and stiffness as the dowel diameter increased. Further work is required to compare the numerical model to experimental results and utilise the model to further optimise the design of DLT members from Irish grown Sitka spruce and CW dowels.

ACKNOWLEDGEMENTS

The authors would like to acknowledge the support and funding of the Department of Agriculture, Food and the Marine's Competitive Research Funding Programmes, Project Ref: 2019R471 (MODCONS).

REFERENCES

[1] Harte AM. Mass timber – the emergence of a modern construction material. J Struct Integr Maint 2017;2:121–32. doi:10.1080/24705314.2017.1354156.

[2] Brandner R, Flatscher G, Ringhofer A, Schickhofer G, Thiel A. Cross laminated timber (CLT): overview and development. Eur J Wood Wood Prod 2016;74:331–51. doi:10.1007/s00107-015-0999-5.

[3] O'Ceallaigh C, Sikora K, Harte AM. The Influence of Panel Lay-Up on the Characteristic Bending and Rolling Shear Strength of CLT. Buildings 2018;8:15. doi:10.3390/buildings8090114.

[4] Schickhofer G, Brandner R, Bauer H. Introduction to CLT - Product Properties, Strength Classes. Stockholm, Sweden: 2016.

[5] Harte A, McPolin D, Sikora K, O'Neill C, O'Ceallaigh C. Irish Timber – Characterisation, Potential and Innovation. Proc. Civ. Eng. Res. Irel., Belfast, 28-29 August, 2014: 2014, p. 63–8.

[6] Harris R, Ringhofer A, Schickhofer G. Focus Solid Timber Solutions - European Conference on Cross Laminated Timber (CLT). The University of Bath, Bath: The University of Bath; 2013.

[7] StructureCraft. Dowel Laminated Timber (DLT) - Design and Profile Guide. USA: StructureCraft; 2019.

[8] Thoma A, Jenny D, Helmreich M, Gandia A, Gramazio F, Kohler M. Cooperative Robotic Fabrication of Timber Dowel Assemblies. Res. Cult. Archit., Berlin, Boston: Birkhäuser; 2019, p. 77–88. doi:10.1515/9783035620238-008.

[9] El-Houjeyri I, Thi VD, Oudjene M, Khelifa M, Rogaume Y, Sotayo A, et al. Experimental investigations on adhesive free laminated oak timber beams and timber-to-timber joints assembled using thermo-mechanically compressed wood dowels. Constr Build Mater 2019;222:288–99.

[10] O'Loinsigh C, Oudjene M, Ait-Aider H, Fanning P, Pizzi A, Shotton E, et al. Experimental study of timber-to-timber composite beam using welded-through wood dowels. Constr Build Mater 2012;36:245–50. doi:10.1016/j.conbuildmat.2012.04.118.

[11] Mehra S, O'Ceallaigh C, Hamid-Lakzaeian F, Guan Z, Harte AM. Evaluation of the structural behaviour of beam-beam connection systems using compressed wood dowels and plates. In. Proc. WCTE 2018 - World Conf. Timber Eng., Seoul, Rep. of Korea, August 20-23, 2018: 2018.

[12] Mehra S, Mohseni I, O'Ceallaigh C, Guan Z, Sotayo A, Harte AM. Moment-rotation behaviour of beam-column connections fastened using compressed wood connectors. SWST 62 nd Int. Conv. Renew. Mater. Wood-based Bioeconomy, 2019, p. 2019.

[13] O'Ceallaigh C, McGetrick P, Harte AM. The Structural Behaviour of Compressed Wood Manufactured using Fast-grown Sitka Spruce. WCTE 2021 - World Conf. Timber Eng., Santiago, Chile: 2021.

[14] Mehra S, O'Ceallaigh C, Sotayo A, Guan Z, Harte AM. Experimental investigation of the moment-rotation behaviour of beam-column connections produced using compressed wood connectors. Constr Build Mater 2022;331:127327. doi:10.1016/j.conbuildmat.2022.127327.

[15] Plowas W, Bell T, Hairstans R, Williamson JB. Understanding the compatibility of UK resource for dowel laminated timber construction. TH Build Constr 2015:1–12.

[16] O'Loinsigh C, Oudjene M, Shotton E, Pizzi A, Fanning P. Mechanical behaviour and 3D stress analysis of multi-layered wooden beams made with welded-through wood dowels. Compos Struct 2012;94:313–21. doi:10.1016/j.compstruct.2011.08.029.

[17] Sotayo A, Bradley D, Bather M, Sareh P, Oudjene M, El-Houjeyri I, et al. Review of state of the art of dowel laminated timber members and densified wood materials as sustainable engineered wood products for construction and building applications. Dev Built Environ 2020;1:100004. doi:10.1016/j.dibe.2019.100004.

[18] Oudjene M, Khelifa M, Segovia C, Pizzi A. Application of numerical modelling to dowel-welded wood joints. J Adhes Sci Technol 2010;24:359–70. doi:10.1163/016942409X12541266699473.

[19] Guan Z, Sotayo A, Oudjene M, Houjeyri I El, Harte A, Mehra S, et al. Development of Adhesive Free Engineered Wood Products – Towards Adhesive Free Timber Buildings. Proc. WCTE 2018 World Conf. Timber Eng. Seoul, Rep. Korea, August 20-23, 2018, 2018.

[20] ETA-13/0785. European Technical Approval. Solid wood slab element - element of dowel jointed timber boards to be used as a structural elements in buildings. ETA-Denmark, Nordhavn, Denmark: 2013.

[21] CEN. EN 408. Timber structures - Structural timber and glued laminated timber - Determination of some physical and mechanical properties. Comité Européen de Normalisation, Brussels, Belgium: 2012.

[22] O'Ceallaigh C, Sikora K, McPolin D, Harte AM. An investigation of the viscoelastic creep behaviour of basalt fibre reinforced timber elements. Constr Build Mater 2018;187:220–30. doi:10.1016/j.conbuildmat.2018.07.193.

[23] O'Ceallaigh C, Sikora K, McPolin D, Harte AM. Modelling the hygro-mechanical creep behaviour of FRP reinforced timber elements. Constr Build Mater 2020;259. doi:10.1016/j.conbuildmat.2020.119899.

[24] O'Ceallaigh C. An Investigation of the Viscoelastic and Mechano-sorptive Creep Behaviour of Reinforced Timber Elements. PhD Thesis, National University of Ireland Galway, 2016.

[25] CEN. EN 338. Structural timber - Strength classes. Comité Européen de Normalisation, Brussels, Belgium; 2016.

[26] Bodig J, Jayne BA. Mechanics of Wood Composites. Reprinted edition. Von Nostrand Reinhold Company, New York, Cincinnati, Toronto 1993.

[27] Conway M, O'Ceallaigh C, Mehra S, Harte AM. Reinforcement of Timber Elements in Compression Perpendicular to the Grain using Compressed Wood Dowels. Civ. Eng. Res. Ireland, CERI 2020. Cork Inst. Technol. 27-28 August, 2020, p. 319–24. doi:https://doi.org/10.13025/sbeg-3p91.

[28] O'Ceallaigh C, Conway M, Mehra S, Harte AM. Numerical Investigation of Reinforcement of Timber Elements in Compression Perpendicular to the Grain using Densified Wood Dowels. Constr Build Mater 2021;288. doi:10.1016/j.conbuildmat.2021.122990.

[29] Conway M, Harte AM, Mehra S, O'Ceallaigh C. Densified Wood Dowel Reinforcement of Timber Perpendicular to the Grain: A Pilot Study. J Struct Integr Maint 2021;6:177–86. doi:10.1080/24705314.2021.1906090.

[30] O'Ceallaigh C, Mohseni I, Mehra S, Harte AM. Numerical Investigation of the Structural Behaviour of Adhesive Free Connections Utilising Modified Wood. WCTE 2021- World Conf. Timber Eng., Chile: 2021.

[31] Namari S, Drosky L, Pudlitz B, Haller P, Sotayo A, Bradley D, et al. Mechanical properties of compressed wood. Constr Build Mater 2021;301. doi:10.1016/j.conbuildmat.2021.124269.

[32] Jung K, Kitamori A, Komatsu K. Evaluation on structural performance of compressed wood as shear dowel. Holzforschung 2008;62:461–7. doi:10.1515/HF.2008.073.

[33] Mehra S, Harte AM, Sotayo A, Guan Z, O'Ceallaigh C. Experimental investigation on the effect of accelerated ageing conditions on the pull-out capacity of compressed wood and hardwood dowel type fasteners. Holzforschung 2021.

[34] Valipour H, Khorsandnia N, Crews K, Palermo A. Numerical modelling of timber/timber-concrete composite frames with ductile jointed connection. Adv Struct Eng 2016. doi:10.1177/1369433215624600.

[35] Kawecki B, Podgórski J. Numerical analysis and its laboratory verification in bending test of glue laminated timber pre-cracked beam. Materials (Basel) 2019;16:1–15. doi:10.3390/ma12060955.

[36] Portioli F, Marmo R, Ceraldi C, Landolfo R. Numerical modeling of connections with timber pegs. 11th World Conf. Timber Eng. 2010, WCTE 2010, vol. 3, 2010, p. 1881–6.

[37] Khorsandnia N, Valipour HR, Crews K. Nonlinear finite element analysis of timber beams and joints using the layered approach and hypoelastic constitutive law. Eng Struct 2013;46:606–14. doi:10.1016/j.engstruct.2012.08.017.

[38] Chybiński M, Polus Ł. Experimental and numerical investigations of aluminium-timber composite beams with bolted connections. Structures 2021;34:1942–60. doi:10.1016/j.istruc.2021.08.111.